Developmental Cell, Vol. 6, 253–268, February, 2004, Copyright ©2004 by Cell Press

Aurora B Regulates MCAK at the Mitotic Centromere

Paul D. Andrews,[1,*] Yulia Ovechkina,[3] Nick Morrice,[2] Michael Wagenbach,[3] Karen Duncan,[1] Linda Wordeman,[3] and Jason R. Swedlow[1]
[1]Division of Gene Regulation and Expression
[2]MRC Protein Phosphorylation Unit
Wellcome Trust Biocentre
University of Dundee
Dow Street
Dundee DD1 5EH
United Kingdom
[3]Department of Physiology and Biophysics
University of Washington School of Medicine
1959 N.E. Pacific Street
Seattle, Washington 98195

Summary

Chromosome orientation and alignment within the mitotic spindle requires the Aurora B protein kinase and the mitotic centromere-associated kinesin (MCAK). Here, we report the regulation of MCAK by Aurora B. Aurora B inhibited MCAK's microtubule depolymerizing activity in vitro, and phospho-mimic (S/E) mutants of MCAK inhibited depolymerization in vivo. Expression of either MCAK (S/E) or MCAK (S/A) mutants increased the frequency of syntelic microtubule-kinetochore attachments and mono-oriented chromosomes. MCAK phosphorylation also regulates MCAK localization: the MCAK (S/E) mutant frequently localized to the inner centromere while the (S/A) mutant concentrated at kinetochores. We also detected two different binding sites for MCAK using FRAP analysis of the different MCAK mutants. Moreover, disruption of Aurora B function by expression of a kinase-dead mutant or RNAi prevented centromeric targeting of MCAK. These results link Aurora B activity to MCAK function, with Aurora B regulating MCAK's activity and its localization at the centromere and kinetochore.

Introduction

Accurate chromosome segregation requires the attachment of microtubules from opposing spindle poles to kinetochores formed on sister chromatids. The Aurora B kinase and its associated binding partners INCENP and survivin play a critical role in this process. Mutations in the yeast Aurora B homolog, Ipl1, generate stably mono-oriented chromosomes that fail to resolve (He et al., 2001; Tanaka et al., 2002). In *Drosophila* and *C. elegans*, Aurora B RNAi cells possess aberrant prometaphase-like mitotic spindles that fail to align their chromosomes on the metaphase plate and subsequently develop significant aneuploidy due to chromosome nondisjunction (Adams et al., 2001; Giet and Glover, 2001; Kaitna et al., 2000). Introduction of dominant-negative mutants of Aurora B or small molecule inhibitors into mammalian cells causes similar phenotypes (Ditchfield et al., 2003; Hauf et al., 2003; Murata-Hori and Wang, 2002). Together, these results suggest that the Aurora B complex plays a critical role in establishing bipolar chromosome attachment and that this function is highly conserved.

Aurora B, INCENP, and survivin all behave as chromosome passenger proteins, localizing between sister centromeres in the inner centromere from late G2 through to metaphase (Andrews et al., 2003; Carmena and Earnshaw, 2003). As chromosome segregation initiates, the complex leaves the inner centromere and concentrates on central spindle microtubules where it functions in cytokinesis. In yeast, the Aurora B/Ipl1p complex phosphorylates a number of inner and outer kinetochore proteins (Biggins et al., 1999; Cheeseman et al., 2002; Westermann et al., 2003). Aurora B also phosphorylates the centromere-specific histone H3 variant CENP-A (Zeitlin et al., 2001), as well as histone H3 localized throughout the chromosome (Hsu et al., 2000; Murnion et al., 2001). The concentration of the Aurora B complex at the inner centromere and its interaction with kinetochore components suggest that it may regulate the interactions between kinetochores and microtubule ends.

One possible substrate for the Aurora B complex is the KinI kinesin MCAK. Unlike conventional kinesins, Kin I family members have their motor domains in the central portion of the molecule and use the hydrolysis of ATP to depolymerize microtubule ends (Desai et al., 1999; Hunter et al., 2003; Hunter and Wordeman, 2000). In *Xenopus* egg extracts, depletion of the *Xenopus* homolog XKCM1 decreases the catastrophe rate of microtubule ends and causes chromosomes to misalign on the mitotic spindle (Walczak et al., 2002, 1996). In mammalian cells, depletion of MCAK by antisense DNA inhibits anaphase A (Maney et al., 1998). MCAK/XKCM1 is localized to centromeres in early prophase and remains there throughout mitosis (Walczak et al., 1996; Wordeman et al., 1999).

A critical unanswered question is how MCAK/XKCM1 activity is regulated. As a regulator of microtubule end catastrophe, soluble MCAK/XKCM1 can affect the average length of spindle microtubules in *Xenopus* egg extracts (Walczak et al., 1996). However, MCAK/XKCM1 also functions during chromosome alignment (Walczak et al., 2002), suggesting that the activity of kinetochore-bound MCAK/XKCM1 might be regulated as chromosomes undergo saltatory motion in prometaphase and metaphase (Rieder and Salmon, 1994; Skibbens et al., 1993). We have examined the functional interactions between Aurora B and MCAK and found that the mitotic Aurora B complex is a critical regulator of MCAK function in vitro and in vivo.

Results

Spatial Distribution of Aurora B and MCAK in the Cell Cycle

Independent immunofluorescence studies have previously shown Aurora B and MCAK localized to centromeres of mammalian chromosomes from late prophase

*Correspondence: p.d.andrews@dundee.ac.uk

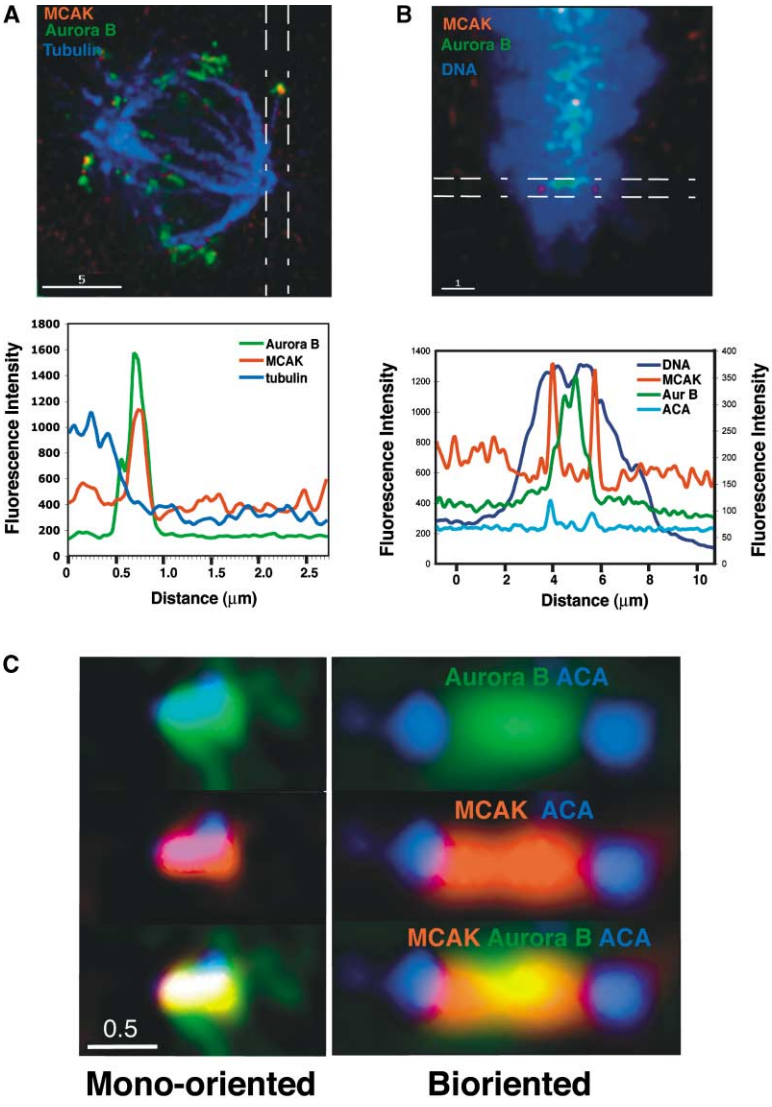

Figure 1. Aurora B and MCAK Localization in HeLa Cells

Prometaphase and metaphase HeLa cells stained for human MCAK, Aurora B, tubulin, and DNA. All images are single optical sections.

(A) In prometaphase mono-oriented chromosomes, Aurora B and MCAK show complete colocalization.

(B) In metaphase bioriented chromosomes under tension, MCAK and Aurora B are largely distinct, with MCAK close to ACA staining and Aurora B concentrated in the inner centromere. Line profiles (lower panel) show the spatial separation of the signals (lower panels).

(C) Differences in MCAK and Aurora B localization in prometaphase at high resolution. Images are from two different chromosomes from the same prometaphase cell. In mono-oriented chromosomes (left), sister centromeres are closely spaced, while in bioriented chromosomes (right) they are separated.

of the cell cycle to until the metaphase-anaphase transition (Andrews et al., 2003; Carmena and Earnshaw, 2003; Maney et al., 1998; Walczak et al., 1996). During anaphase and telophase, MCAK remains centromere-associated while Aurora B relocalizes to the spindle midzone. We re-examined the localization of Aurora B and MCAK during prometaphase and metaphase in mitotic HeLa cells. During prometaphase, Aurora B and MCAK colocalized in unattached or mono-oriented (i.e., attached to kinetochore fibers from one pole only) chromosomes (Figure 1A). The ACA antigen also localized with Aurora B and MCAK. By contrast, in chromosomes aligned along the metaphase plate, MCAK concentrated at two sites that partially colocalized with ACA staining but that were distinct from the strictly inner-centromeric localization of Aurora B (Figure 1B). MCAK and Aurora B also colocalized in cells treated with nocodozole and taxol (data not shown). To further define when the relative localization of Aurora B and MCAK changed, we examined prometaphase at high resolution (Figure 1C) and found two distinct types of Aurora B/MCAK colocalization. In centromeres under tension (as judged by the distance between ACA staining sites [Waters et al., 1996]), Aurora B and MCAK were only partially colocalized, whereas centromeres not under tension still showed significant colocalization. The localization of MCAK is therefore dynamic, initially colocalizing with Aurora B following assembly of mitotic chromosomes, but then becoming distinct from Aurora B as tension develops across sister kinetochores.

Aurora B Phosphorylates MCAK In Vitro

We next tested whether the Aurora B complex might phosphorylate MCAK in vitro. Recombinant full-length MCAK was incubated in the presence of ^{32}P-γ-ATP and mitotic Aurora B complex isolated from *Xenopus* chromosomes. We chose this strategy because we have failed to produce recombinant *Xenopus* Aurora B complex with the same activity and properties as the mitotic complex (Murnion et al., 2001; data not shown). Figure 2A shows that MCAK was phosphorylated in vitro by mitotic Aurora B complex. Kinase activity was not detected toward MCAK using interphase Aurora B or control IgG beads. To confirm this result, we incubated a

mixture of recombinant forms of Ipl1p and Sli15p, the budding yeast orthologs of Aurora B and INCENP, respectively, with recombinant MCAK. Mixing Sli15p and Ipl1p stimulates Ipl1p kinase activity (Kang et al., 2001). This mixture produced high levels of MCAK phosphorylation (Figure 2B). These results suggested MCAK is phosphorylated by Aurora B in vitro.

We next identified the sites in MCAK phosphorylated by the mitotic Aurora B complex. We incubated recombinant MCAK with interphase or mitotic Aurora B complex and ^{32}P-γ-ATP, or with recombinant yeast Ipl1p/Sli15p complex, and then analyzed ^{32}P-labeled tryptic peptides from MCAK by reverse-phase HPLC. The phosphopeptides generated with mitotic Aurora B were similar to those obtained with recombinant yeast Ipl1p/Sli15p (Supplemental Figure S1 [http://www.developmentalcell.com/cgi/content/full/6/2/253/DC1). As expected from MCAK's primary amino acid sequence, trypsin generated a significant number of very short MCAK peptides, many of which were radiolabeled. To simplify the profile, we used Lys-C for proteolytic cleavage. Analysis of Lys-C-digested MCAK phosphorylated by Aurora B produced three distinct peaks of radioactivity (Figure 2C), which were then characterized using a combination of Edman sequencing and MALDI-TOF (Figure 2D). Peak 1 corresponded to phosphorylation at Ser92, while Peak 2 corresponded to phosphorylation at Ser186. Peak 3 corresponded to phosphorylation at Ser106, Ser108, and Ser112, but MALDI-TOF analysis showed that all peptides in this fraction were monophosphorylated, indicating that only one of the three serines was phosphorylated in any single peptide. Comparison of the integrated peak heights from the HPLC analysis indicates that Peak 3 sites are less efficiently phosphorylated than Peak 1 and Peak 2 sites.

The Aurora B sites in MCAK conform to the consensus sequence derived from known Aurora B substrates (Figure 2E; Cheeseman et al., 2002). All three sites in MCAK are preceded by one or more K or R residues and often, but not always, are followed by a hydrophobic residue. Alignment of the N termini of MCAK and its orthologs with the closely related Kif2 kinesins reveals that the Aurora B phosphorylation sites identified here are highly conserved in all KinI kinesins (Figure 2F). The Kif2 kinesins regulate cytoplasmic microtubules during neurite extension (Homma et al., 2003). The conservation of sites in the Kif2's with those identified in MCAK suggests a conserved mechanism of regulating the activity of these enzymes.

Aurora B Phosphorylates MCAK In Vivo

In order to test the phosphorylation of MCAK in cells, we used a synthetic phosphopeptide derived from phosphorylation Site 1 in human MCAK (Figure 2E) to generate novel anti-MCAK antibodies. We used repeated rounds of affinity purification to isolate antibodies that specifically recognized MCAK phosphorylated on Ser92 (α-P-Ser92) and antibodies that recognized both dephosphorylated and phosphorylated MCAK (α-Ser92). Figure 3A shows that α-P-Ser92 only recognizes the phosphopeptide antigen, but not the desphosphopeptide in an ELISA assay, while α-Ser92 recognizes both forms of the peptide. In addition, α-P-Ser92 only recognized MCAK on immunoblots after phosphorylation with recombinant Ipli1p/Sli15p (Figure 3B). By contrast, control antibodies recognized both nonphosphorylated and phosphorylated forms of MCAK on the same blot. Together, these results suggest that the α-P-Ser92 antibody recognizes phosphorylated MCAK.

To examine the phosphorylation state of MCAK in cells, we performed immunoblots of lysates from control and nocodozole-arrested HeLa cells with α-P-Ser92. Figure 3C shows a series of slow-migrating forms of MCAK enriched in nocodozole-arrested lysates. α-P-Ser92 only recognized the slowest migrating bands, and showed highest reactivity after nocodozole arrest, suggesting that MCAK phosphorylation is highest in mitotic cells. Localization of MCAK phosphorylation by immunofluorescence revealed that α-P-Ser92 recognized centromeric MCAK in prometaphase cells (Figure 3D). We also noted abundant α-P-Ser92 signal throughout the cell, suggesting that cytoplasmic MCAK may also be phosphorylated at Ser92. Both the centromeric and cytoplasmic signals were blocked with the P-Ser92 peptide but not the Ser92 peptide, confirming the specificity of α-P-Ser92 in cells.

While we noted an increase in mitotic MCAK phosphorylation both on immunoblots and by immunofluorescence (Figures 3C and 3D), closer examination revealed differences in MCAK phosphorylation across the centromere. In prometaphase and metaphase cells transfected with wtMCAK-GFP, we detected similar amounts of MCAK at sister centromeres and kinetochores, yet significant differences in the level of α-P-Ser92 staining (Figure 3E). These differences in antibody staining may occur due to changes in antigen accessibility or because of differences in MCAK phosphorylation. We have never observed systematic asymmetry in MCAK staining between sister centromeres or kinetochores with other MCAK antibodies (see Figure 1), suggesting that the phosphorylation state of MCAK at centromeres and kinetochores at Ser92 may be dynamic.

We next asked whether in vivo phosphorylation of MCAK at Ser92 was dependent on Aurora B. HeLa cells were treated with nocodozole and transfected with a siRNA targeted to human Aurora B (see Experimental Procedures). Aurora B depletion was assayed both biochemically (Supplemental Figure S2) and by immunofluorescence in single cells. In cells depleted of Aurora B, the phospho-specific α-P-Ser92 antibody reactivity at the centromere was largely abolished (Figure 3F). By contrast, reactivity of the α-Ser92 antibody, which recognizes both phosphorylated and nonphosphorylated MCAK (Figure 3B), remained unchanged. This suggests that phosphorylation of centromeric MCAK at Ser92, a major site of MCAK phosphorylation in vitro, also occurs in vivo and is dependent on Aurora B. In addition, after depletion of Aurora B by RNAi, the migration of MCAK on a 2D gel changes from pI $\sim$6.5 to pI $\sim$8.5, consistent with a loss of phosphorylation (Supplemental Figure S2).

Aurora B Phosphorylation Inhibits the Activity of MCAK

We next assayed whether the phosphorylation of MCAK by Aurora B affected MCAK's depolymerization activity in vitro using a microtubule sedimentation assay. In the absence of MCAK, the vast majority of tubulin from

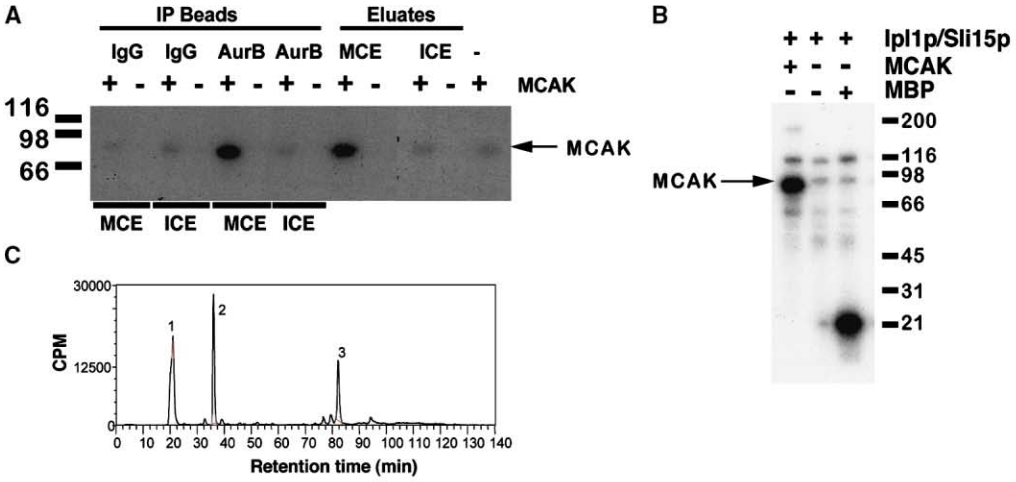

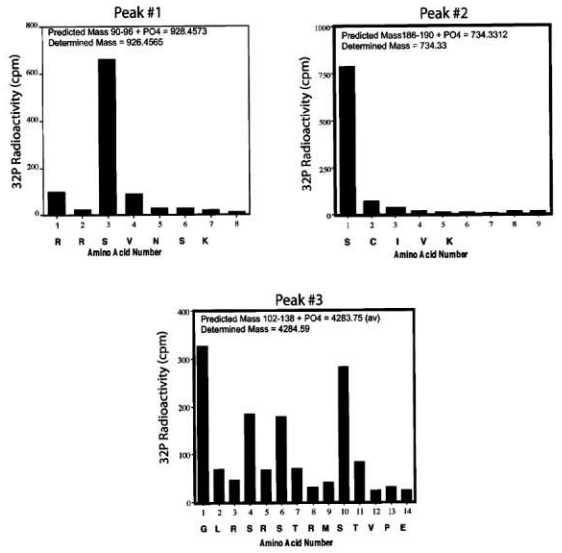

E

```
CgMCAK          87  KQKRRSVNSKI
               101  KEGLRSRSTRM
               181  PARRKSCIVKE

Histone H3       5  QTARKSTGGKA
                23  KAARKSAPATG

HsCENP-A         2  GPRRRSRKPEA

ScDam1p         20  TEYRLSIGSAP
               257  KLRRKSILHTI
               267  HTIRNSIASGA
               292  PNNRISLGSGA

Spc34p         199  NQRRKTIFVED

Ndc80p         100  SVSRLSINQLG

Ask1p          200  RKRKISLLLQQ
```

F

```
                                Peak 1                          - Peak3 -
CgMCAK      77 LPLQENVTVPKQKRRSVNSKIPAPKEG---------------LRSRSTRMSTVPEVRIATQENEMEVELPV..
HsMCAK      80 LPLQENVTIQKQKRRSVNSKIPAPKES---------------LRSRSTRMSTVSELRITAQENDMEVELPA..
RnKRP2      26 --TATAGERNHPKAKTQVRQLQNSRS-------------KRRPSKRSTRISTVSEVRIPAQENEMEVELPVS..
XlKCM1      79 MPPQRNVSSQNHKRKTI-SKIPAPKEVAAKNSLLSESGAQSVLRERSTRMTAIHETLPYENEMEAE-STPL..
HsKIF2      52 PASSAKVNKIVKNRRTVASIKNDPPSRDN-----------RVVGSARARPSQFPEQSSSAQQNGSVSDISPV..
MmKIF2      51 -SSSSKVNKIVKNRRTVAAVKNDPPPRDN-----------RVVGSARARPSQLPEQSSSAQQNGSVSDISPV..
MmKIF2b     51 PSSSSKVNKIVKNRRTVAARAVKNDPPPR-----------DNRVVGSARPSQLPEQSSSAQQN---------..
XKIF2       76 PAPTTKVNKIVKNRRTVAPVKNETPAKDN---------RVAAVGSARARPIQPIEQSASRQQNGSVSDISPD..

                                                                Peak 2
CgMCAK         156 ELPLSMVSEEAEEQVHPTRSTSSAN--------PARRKSCIVKEMEKMKNKREEKRAQ
HsMCAK         159 EIPLRMVSEEMEEQVHSIRGSSSANPV-----NSVRRKSCLVKEVEKMKNKREEKKAQ
RnKRP2         105 ELPLLMISEEAEEQAHSTRSTSSANPG-----NSVRRKSCIVKEMEKMKNKREEKRAQ
XlKCM1         158 RSRSTKVSIAEEPRLQTRISEIVEESLPSGRNNQGRRKSNIVKEMEKMKNKREEQRAQ
HsKIF2         125 ---------------------------------PSRRKSNCVKEVEKLQEKREKRRLQ
MmKIF2         124 ---------------------------------PSRRKSNCVKEVEKLQEKREKRRLQ
MmKIF2b        106 ---------------------------------ARRKSNCVKEVEKLQEKREKRRLQ
XKIF2          151 --------------------------------ASRRKSNCVKEVEKLQEKRERRRLQ
DmKlp10A       180 AAASAGPAAQGVATAATTQGAGG----------ASTRRSHALKEVERLKENREKRRAR
CfDSK           24 ----------------------------MNAANRRKSTSTVGITGRKDATRMKIEQ
```

taxol-stabilized microtubules sediments in the pellet (Figure 4A, "P"; lanes 5–8). MCAK incubated with control beads retained full depolymerization activity (Figure 4A, "S"; lanes 3 and 4). In contrast, the activity of MCAK phosphorylated by the immunopurified Aurora B complex was significantly reduced (Figure 4A, lanes 1 and 2), suggesting that in vitro phosphorylation by Aurora B inhibits the microtubule depolymerizing activity of MCAK. Similarly, a mixture of recombinant Ipl1p and Sli15p (Kang et al., 2001) also reduced MCAK's in vitro microtubule depolymerizing activity (Figure 4B, lanes 1 and 2).

To assess the effect of MCAK phosphorylation in vivo, we transfected HeLa cells with GFP-MCAK constructs bearing mutations in the phosphorylation sites we identified in Figure 2 and then measured the amount of polymerized tubulin present in transfected cells by immunofluorescence (Ovechkina et al., 2002). Transfection of GFP fused to wild-type MCAK (wtMCAK) efficiently depolymerized most of the microtubules in the cell (Figures 4C and 4D). All constructs bearing single S→A or S→E mutations efficiently depolymerized microtubules in this in vivo assay (data not shown). In addition, transfection with either double S→A mutants or the quintuple S92A/S106A/S108A/S112A/S186A MCAK, "AAAAA-MCAK," caused no detectable effect on microtubule depolymerization. In contrast, cells transfected with either double S→E mutations or the quintuple S92E/S106E/S108E/S112E/S186E MCAK, "EEEEE-MCAK," contained significantly more tubulin polymer, suggesting that MCAK proteins bearing these phosphorylation-mimicking mutations are less active than wtMCAK or the various S→A mutants. Together, these in vitro and in vivo results suggest that phosphorylation inhibits MCAK catalytic activity.

Phenotypes and Localization of MCAK Phosphorylation-Site Mutants

We next assessed the effect of introducing MCAK constructs bearing mutations in the Aurora B phosphorylation sites on the mitotic spindle. In Figures 5A–5C, we show four representative examples of each construct. HeLa cells transfected with wtMCAK fused to GFP formed normal mitotic spindles, with apparently bioriented chromosomes and GFP-MCAK localization indistinguishable from the endogenous protein (Figure 5C). Transfection of cells with either AAAAA-MCAK (Figure 5A), or EEEEE-MCAK (Figure 5B), produced aberrant mitotic figures with frequent misoriented chromosomes. In cells expressing AAAAA-MCAK, we observe a significant increase in monopolar chromosomes and chromosomes with apparently syntelic (both kinetochores attached to same pole) or monotelic kinetochore-microtubule attachments (one kinetochore attached to microtubules from one pole). Expression of EEEEE-MCAK caused a high frequency of mitotic figures with poorly aligned chromosomes that were often clustered on the periphery of the mitotic spindle (Figure 5B). Cytological analysis of mitotic progression revealed that EEEEE-MCAK increased the frequency of prometaphase figures, whereas AAAAA-MCAK increased the frequency of metaphase figures (Figure 5D).

Since MCAK localization normally changes from the inner centromere to the inner kinetochore during prometaphase (Figure 1), we determined the localization of the different MCAK mutants. AAAAA-MCAK often localized away from the inner centromere, closer to ACA staining, even in prometaphase figures where MCAK is normally localized to the inner centromere (Figure 5E, see also Figure 1). In contrast, EEEEE-MCAK localized to the inner centromere even in metaphase chromosomes where MCAK normally localizes to the inner kinetochore (Figure 5E). The visual impression gained in Figure 5E is quantified in Figure 5F. We conclude that multiple MCAK binding sites may be present on chromosomes and MCAK's association with these sites depends on its phosphorylation state.

We next used fluorescence recovery after photobleaching (FRAP) of the MCAK mutants to determine if the phosphorylation state of MCAK affects its association with centromeres and kinetochores in living cells. We bleached GFP-MCAK and then examined the recovery of fluorescence, to assay the association of the different MCAK mutants with centromeres and kinetochores. wtMCAK, EEEEE-MCAK, and AAAAA-MCAK all recovered rapidly, although the recovery rate for AAAAA-MCAK was noticeably slower (Figures 6A–6C). We noted that wtMCAK recovers more slowly on aligned chromosomes (Figure 6D, blue bars) than on unaligned chromosomes (Figure 6D, red bars), suggesting a change in the affinity of MCAK for the centromere/kinetochore as chromosomes align. Although we do not have sufficient resolution or fiduciary marks in this live cell experiment to distinguish centromere- and kinetochore-associated populations of MCAK, our localization data

Figure 2. Aurora B Phosphorylation of MCAK In Vitro

(A) Autoradiograph of SDS-PAGE gel of recombinant full-length MCAK phosphorylated in the presence of ^{32}P-ATP using Aurora B immunoprecipitated from *Xenopus* mitotic chromosomal eluate (MCE), Aurora B from *Xenopus* interphase chromosomal eluate (ICE), control immunoprecipitations from MCE and ICE, or crude MCE or ICE alone. As a further control, MCAK alone was incubated in kinase buffer in the presence of ^{32}P-ATP.

(B) Autoradiograph of SDS-PAGE gel of recombinant full-length MCAK phosphorylated in the presence of ^{32}P-ATP using active recombinant Ipl1p/Sli15 complex. Myelin basic protein is included as a control (right lane). Weakly phosphorylated bands present in all lanes are derived from Sli15p.

(C) Recombinant hamster MCAK was phosphorylated with mitotic Aurora B and digested with LysC endoproteinase. Peptides were separated by RP-HPLC and the three radioactive peptides peaks isolated.

(D) Radiolabeled phosphopeptides were identified by MALDI-TOF (see Supplemental Table S1) and the position of the phosphorylated residue(s) determined by solid-phase Edman sequencing, monitoring release of radioactivity at each cycle.

(E) Comparison of MCAK phosphorylation sites with known Aurora B substrates (Cheeseman et al., 2002).

(F) Alignment of conserved Aurora B phosphorylation sites (red), and basic (green) and hydrophobic residues (blue) in KinI kinesins. The alignment of *Xenopus* XKCM1 with its mammalian orthologs in the region of Site 2 differs from that previously published (Walczak et al., 2002).

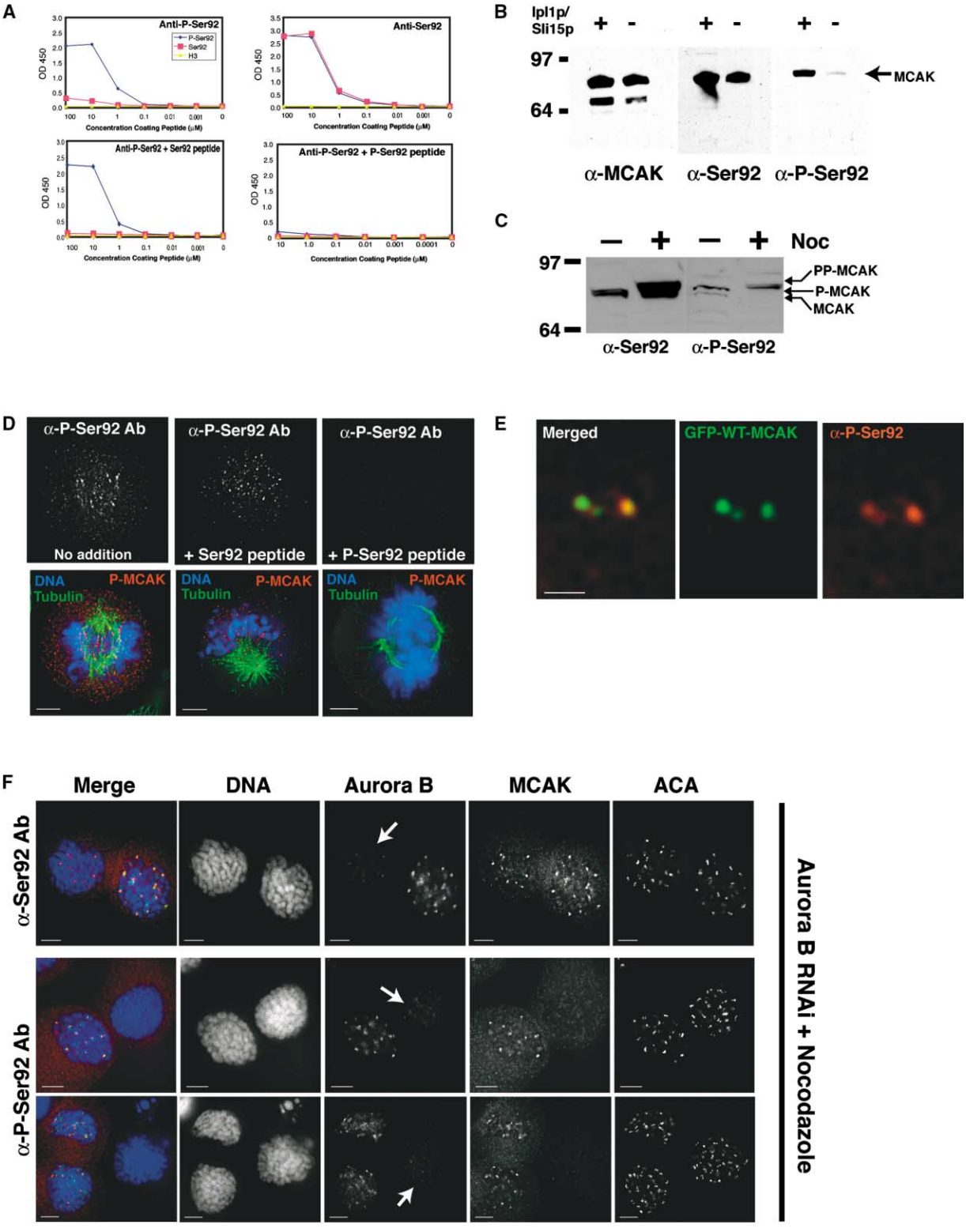

Figure 3. α-Phospho-Ser92 Antibodies Show Aurora B-Dependent MCAK Phosphorylation In Vivo

(A) Specificity tests of affinity-purified α-P-Ser92 and α-Ser92 antibodies. Upper panels, ELISAs with P-Ser92 peptide (blue), Ser92 peptide (pink), Histone H3 Ser10 peptide (yellow). Lower panels, ELISAs after preblocking antibodies.

(B) α-P-Ser92 antibody detects full-length recombinant MCAK only when MCAK has been phosphorylated in vitro with Ipl1p/Sli15p (right-hand panel). Control antibodies are polyclonal sheep α-MCAK Ab and α-Ser92.

(C) α-P-Ser92 antibody recognizes only lower mobility MCAK species in Western blots of whole-cell extracts of asynchronous HeLa cells or HeLa cells arrested with nocodazole for 16 hr. α-Ser92 antibody reacts with all MCAK species on identical blots.

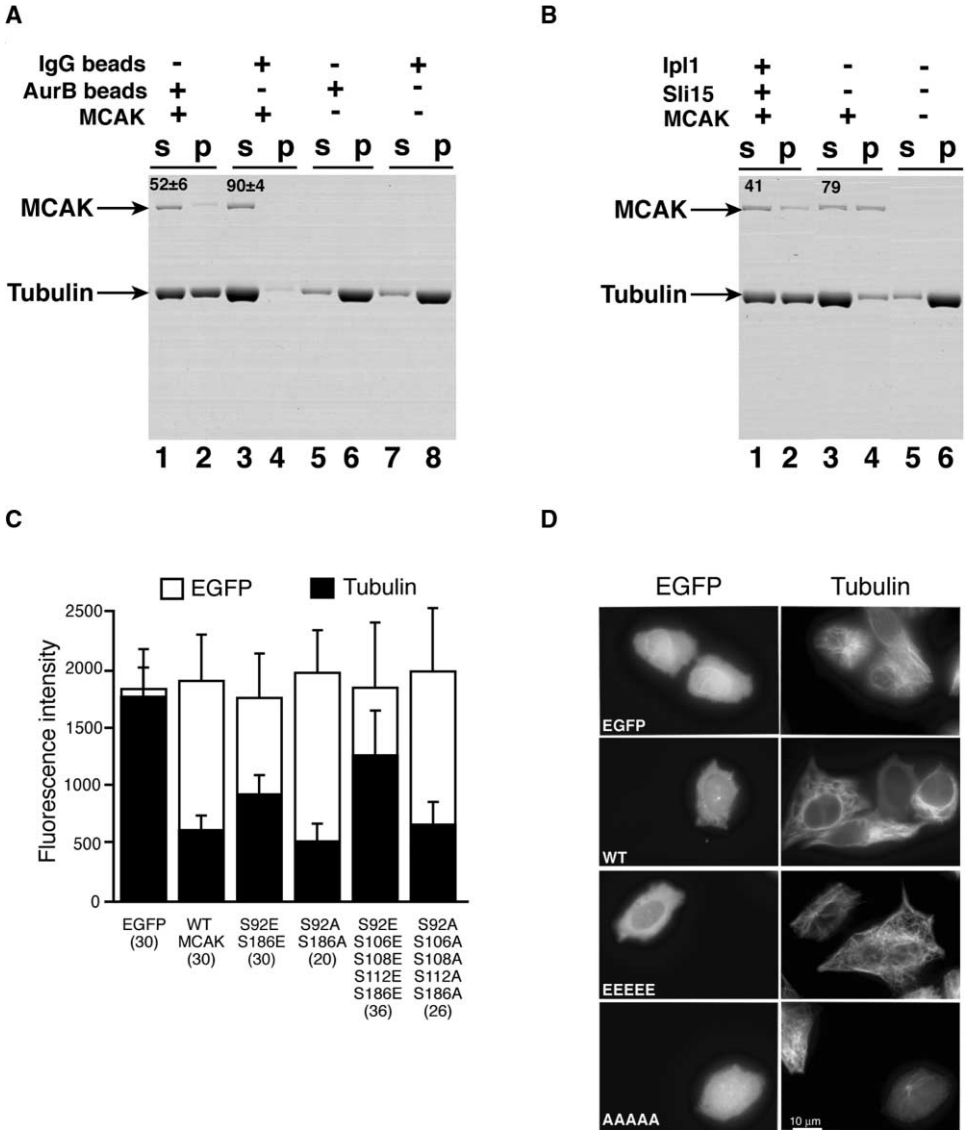

Figure 4. Aurora B-Mediated Phosphorylation Inhibits the Microtubule Depolymerization Activity of MCAK In Vitro and In Vivo

MCAK was incubated with Aurora B complex immunoprecipitated from MCE with α-Aurora B beads or with control beads (A) or with recombinant Ipl1p-Sli15p complex.

(B) Taxol-stabilized microtubules (1500 nM) were added to the phosphorylation reactions containing 24 nM MCAK dimer and 1 mM ATP and incubated for 10 min at RT and then analyzed by sedimentation assay. % tubulin released into the supernatant is shown as mean ± σ (N = 3). In each case, the upper band on the gel is MCAK and the lower band is tubulin.

(C) In vivo analysis of GFP-MCAK and phosphorylation site mutants. CHO cells were transfected with MCAK or MCAK mutants and then fixed and stained for tubulin. Cells were quantified for microtubule loss as described previously (Ovechkina et al., 2002). Total MCAK protein was measured by GFP fluorescence (white bars). Total tubulin polymer was measured by indirect immunofluorescence (black bars).

(D) Images of typical GFP-MCAK-transfected CHO cells used for measurements shown in (C).

(D) α-P-Ser92 antibody recognizes centromeric MCAK in fixed HeLa cells (left). Upper panels are grayscale images of P-Ser92 staining; lower panels are merged images showing DNA (blue), tubulin (green), and P-Ser92 (red). Preblocking with Ser92 peptide had no effect on MCAK reactivity (middle), whereas preblocking with P-Ser92 abolished MCAK reactivity (right).

(E) HeLa cells transfected with wtMCAK-GFP were fixed and stained with α-P-Ser92. P-Ser92 can be detected asymmetrically across sister centromeres/kinetochores. Scale 1 μm.

(F) Aurora B-dependent phosphorylation of MCAK at Ser92. HeLa cells were treated simultaneously with nocodazole (to prevent MCAK delocalization; see text and Figure 7) and Aurora B siRNA (see Experimental Procedures), for 16 hr. Cells were fixed and stained for DAPI (blue), Aurora B (green), MCAK (red; either α-Ser92 or α-P-Ser92), and ACA (not shown on merged image, far right-hand panel in grayscale). Arrows indicate Aurora B-depleted cells. α-P-Ser92 staining is lost in cells depleted of Aurora B while α-Ser92 is not affected. Scale, 5 μm.

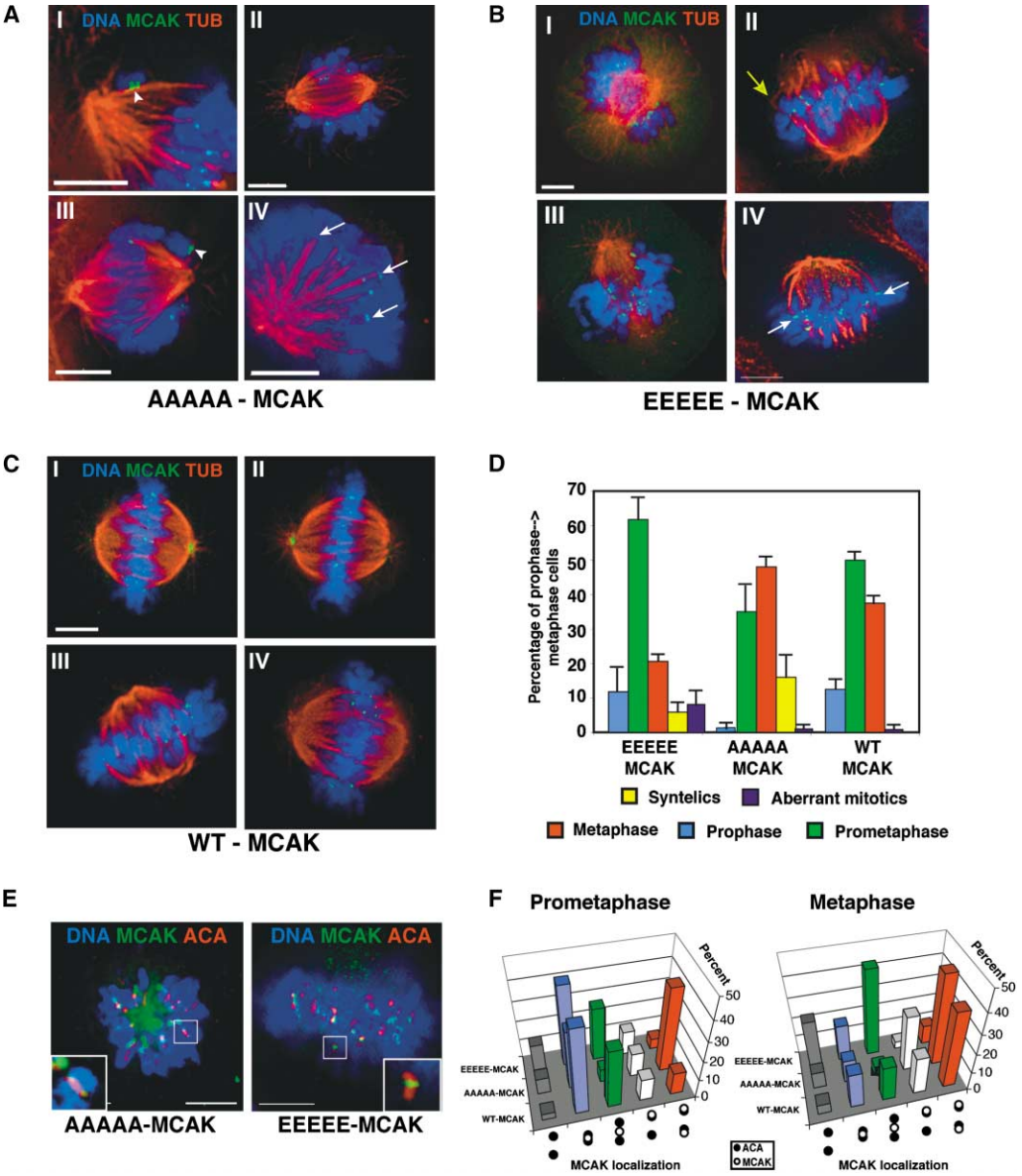

Figure 5. Expression of Phosphorylation-Site Mutants Causes Aberrant Mitotic Phenotypes

HeLa cells transfected with wtMCAK and mutant MCAK plasmids were fixed and stained for tubulin (red) and DNA (blue).

(A) AAAAA-MCAK expression causes accumulation of cells with monopolar chromosomes (arrowheads; panels I–III) and syntelic attachments (arrows; panel IV).

(B) EEEEE-MCAK expression causes aberrant metaphase figures reminiscent of Aurora B or BubRI RNAi (this study; Ditchfield et al., 2003; Hauf et al., 2003) where chromosomes are clustered around a bipolar spindle (panels I and III) as well as irregularly formed mitotic spindles (panel II; yellow arrow) and syntelic attachments (panel IV; arrows).

(C) wtMCAK expression results in normal metaphase figures.

(D) Analysis of cell cycle position and spindle phenotypes after expression of different forms of MCAK.

(E) Localization of MCAK mutants (green) with respect to ACA staining (red) and DNA (blue). AAAAA-MCAK was found mainly to reside outside the ACA-stained region even in prometaphase (see inset). EEEEE-MCAK mainly is found between ACA-pairs even in metaphase cells (see inset).

(F) Quantitation of MCAK localization using ACA antigen staining as a fiduciary marker. The results shown are the average of two experiments (N = 60 cells). MCAK was categorized as either absent from ACA domains; overlapping with ACA where sister centromeres are not under tension; between separated ACA pairs in sisters under tension; overlapping or distal to separated ACA pairs, but asymmetrically localized; or overlapping with separated ACA pairs, but symmetrically localized. In prometaphase, AAAAA-MCAK is predominantly localized distal or overlapping with separated ACA pairs. In metaphase, EEEEE-MCAK is predominantly localized in between ACA pairs.

(Figure 1) suggest that this difference in MCAK association mirrors a difference in localization. We were unable to find a large number of EEEEE-MCAK transfected cells that successfully entered mitosis, but those we studied showed a less pronounced difference between aligned and unaligned chromosomes (Figure 6D). This result, together with EEEEE-MCAK's preferential localization to the inner centromere in fixed cells (Figure 5E) and

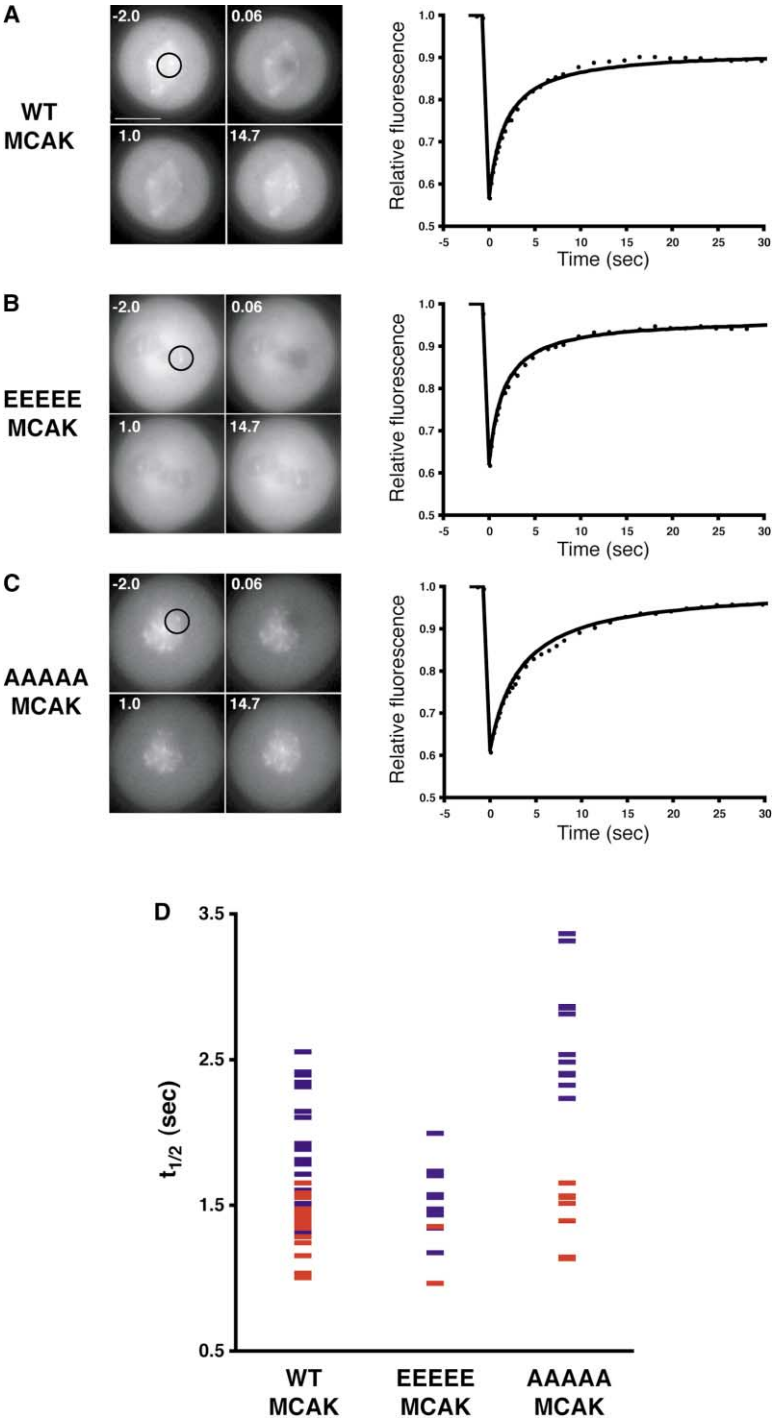

Figure 6. FRAP Analysis of Association of wtMCAK and Phosphorylation-Site Mutants

(A–C) Images before bleaching (−2.0 s), immediately after the photobleach event (0.06 s), during recovery (1.0 s), and later in the time course (14.7 s). Graphs show percent fluorescence recovery versus time for each protein. Dotted lines show the measured data; solid lines show the modeled recovery. (A) wtMCAK. (B) EEEEE-MCAK. (C) AAAAA-MCAK. AAAAA-MCAK displays a longer recovery time than for wild-type or the EEEEE mutant.

(D) Scatter plot of $t_{1/2}$ (horizontal lines) for wtMCAK and mutant MCAKs. Results from aligned centromeres are shown in blue and for unaligned centromeres in red. AAAAA-MCAK recovery $t_{1/2}$s for aligned chromosomes are significantly longer than for wtMCAK or EEEEE-MCAK.

wtMCAK's observed behavior in fixed cells, leads us to speculate that EEEEE-MCAK's faster recovery time is due to its inner-centromeric localization. By contrast, AAAAA-MCAK on aligned chromosomes clearly showed a significantly slower fluorescence recovery rate compared to wtMCAK (Figure 6D). Consistent with AAAAA-MCAK's localization distal to the inner centromere in fixed cells (Figure 5E), our FRAP data suggest the presence of a second MCAK binding site. We therefore postulate the existence of at least two different binding sites for MCAK on chromosomes, whose properties are differentially sensitive to the phosphorylation state of MCAK.

Aurora B Disruption Delocalizes MCAK from Centromeres

Aurora B is required for the localization of dynein, CENP-E, and BubR1 and therefore is a critical regulator of kinetochore function (Ditchfield et al., 2003; Hauf et al., 2003; Murata-Hori et al., 2002). To determine if Aurora

B is required for MCAK localization, we transiently expressed the "kinase-dead" KR mutant of Aurora B, which causes defects in chromosome movement, spindle structure, and dynein/CENP-E localization (Murata-Hori et al., 2002). Cells were transfected with CFP fused to either wt Aurora B or Aurora B (KR) and cotransfected with YFP-MCAK (YFP-FL MCAK) or a construct bearing a deletion of the MCAK motor domain (YFP-ML MCAK; Ovechkina et al., 2002). After transfection with CFP-Aurora B, YFP-FL MCAK localization was indistinguishable from the endogenous protein (Figure 7A). In cells transfected with CFP-Aurora B (KR), YFP-FL MCAK was not concentrated at the inner centromere in either prometaphase or metaphase cells, but was found in the cytoplasm and on the spindle and spindle poles (Figure 7A). A similar effect was observed on endogenous MCAK (data not shown). YFP-ML MCAK was also largely delocalized by CFP-Aurora B (KR) (Figure 7A), but a relatively small population did appear to remain associated with centromeres/kinetochores, the significance of which is currently unclear. These results suggest that Aurora B kinase activity is required for inner centromere targeting of MCAK and that this localization is largely independent of the MCAK motor domain and hence the microtubule depolymerization activity of MCAK.

To confirm our observations with the Aurora B (KR) mutant, we depleted Aurora B by RNAi in HeLa cells and assayed MCAK localization. Figure 7B shows representative prometaphase and metaphase cells from four independent experiments, 12–18 hr posttransfection using Aurora B siRNA or control (scrambled) siRNA duplexes. Aurora B and MCAK levels were quantified in single cells using digital fluorescence imaging (see Experimental Procedures) and in cell lysates by immunoblotting (see Supplemental Figure S2). In Aurora B-depleted cells, we detected no significant change in total cellular MCAK (Figure 7B; also see Supplemental Figure S2). However, after Aurora B depletion, MCAK was no longer concentrated at the inner centromere/kinetochore, but instead was localized throughout the cytoplasm and on the mitotic spindle.

Previous work has shown that the loss of CENP-E and dynein from kinetochores after expression of Aurora B (KR) depends on the presence of microtubules (Murata-Hori et al., 2002). To determine if MCAK's behavior is similar, we added nocodozole to cells after transfection with Aurora B siRNA or Aurora B (KR) cDNA. In cells depleted of Aurora B (Figure 3F) or expressing Aurora B (KR) (data not shown), MCAK still localized to centromeres. We conclude that MCAK's dependence on Aurora B for localization is likely to be similar to other critical kinetochore effectors.

Interfering with Aurora B function causes defects in spindle morphology and chromosome alignment on the metaphase plate (Figure 7C; Andrews et al., 2003; Carmena and Earnshaw, 2003). A chromosome alignment defect was also observed after microinjection of anti-XKCM1 antibodies into mitotic cells (Kline-Smith and Walczak, 2002). To determine if Aurora B RNAi affected microtubule stability within the mitotic spindle, we measured the amount of tubulin polymer at kinetochores by immunofluorescence. Tubulin polymer at kinetochores increased significantly after Aurora B RNAi (Figure 7D), suggesting increased microtubule stability at the kinetochore in the absence of Aurora B and MCAK. By contrast, there was no detectable difference between control RNAi and Aurora B RNAi cells in the total amount of tubulin polymer in mitotic spindles (data not shown). This suggests that delocalized MCAK did not significantly change the global level of tubulin polymer. The proportion of MCAK localized to centromeres in normal mitotic cells represented 33.5 $\pm$ 4.9% of the total cellular MCAK. It seems unlikely that this population, if released into the cytoplasm, would produce a significant change in tubulin polymer levels. Finally, Aurora B RNAi leads to a significant decrease in average centromere-centromere distances compared to control cells, most likely because loss of Aurora B delocalizes MCAK and other factors required for force generation at the kinetochore. The observed decrease in tension after Aurora B depletion is significant, but less than in taxol-treated HeLa cells (see Figure 7E, legend). This partial relief of tension may be due to presence of other kinetochore factors that engage microtubules, or alternatively that residual MCAK generates this result.

Discussion

In this study, we present evidence that the centromeric KinI kinesin MCAK is a substrate for the Aurora B protein kinase during mitosis. Aurora B phosphorylated five conserved serines in the N terminus of MCAK in vitro. A phospho-specific antibody against one of these sites demonstrated Aurora B-dependent MCAK phosphorylation in vivo. Phosphorylation by Aurora B inhibits MCAK's microtubule depolymerizing activity in vitro, and mutagenesis of MCAK phosphorylation sites inhibits the activity of MCAK in vivo. Aurora B and MCAK colocalize on mitotic centromeres before establishment of bipolar attachment, but become spatially separated when centromeres are under tension at metaphase. The phosphorylation-site mutants concentrate at different locations, either within the inner centromere or at the inner kinetochore, and their expression in cells leads to defects in chromosome biorientation. Disruption of Aurora B function decreases MCAK phosphorylation and leads to a microtubule-dependent loss of MCAK from the inner centromere, increased kinetochore microtubule density, and decreased tension across sister centromeres. These data establish a direct link between Aurora B activity and MCAK function at the centromere and kinetochore.

MCAK Is Phosphorylated In Vitro and In Vivo by Aurora B

Our results demonstrate the phosphorylation of a KinI kinesin and identify MCAK as a critical downstream effector of the Aurora B kinase. MCAK was phosphorylated by Aurora B at two sites in the N terminus and one in the neck region. These sites are conserved in most KinI kinesins and represent good consensus Aurora B phosphorylation sites. Using a phospho-specific antibody, we demonstrated that Ser92 is phosphorylated in vivo, in an Aurora B-dependent manner. Interestingly, we detected asymmetry in phospho-specific antibody

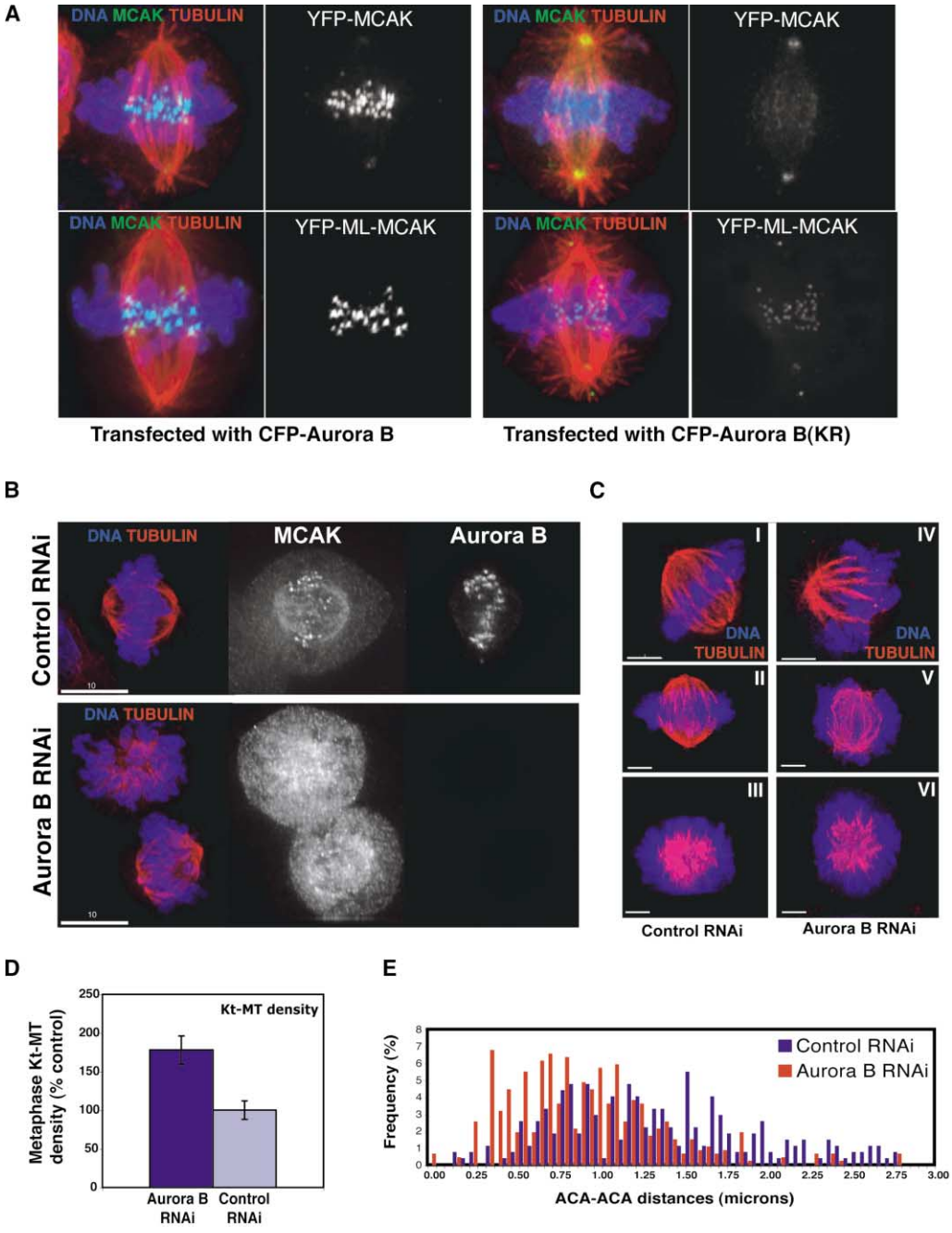

Figure 7. Disruption of Aurora B Function Delocalizes MCAK

(A) Kinase-dead Aurora B (KR) mutant expression results in loss of MCAK from centromeres. CHO cells were transfected with CFP-Aurora B (left) or CFP-Aurora B (KR) (right). Tubulin (red), YFP-MCAK or YFP-motorless (ML) MCAK (green), and DNA (blue). In all panels, CFP-Aurora B has been omitted for clarity. Images are maximum intensity projections of deconvolved 3D data sets.

(B) Aurora B RNAi causes MCAK delocalization from the inner centromere. Tubulin (red), DNA (blue). Top, control RNAi-treated mitotic cell. Bottom, Aurora B RNAi-treated cells. Images are single optical sections of 3D deconvolved data sets acquired under identical conditions and scaled identically.

(C) Spindle structure is aberrant in Aurora B RNAi cells. Aurora B-depleted cells were stained for Aurora B (not shown), tubulin (red), and DNA (blue). Maximum-intensity volume projections were generated from 3D deconvolved data sets. Images show typical spindles for control cells (left panel) or Aurora B RNAi cells (right panel) viewed from two different angles; the lower image is rotated about the *x* axis by 90°.

(D) Aurora B RNAi increases density of microtubules at kinetochores. Graph shows mean $\pm$ σ of total background-corrected fluorescence in a 9 $\times$ 10 pixel box located adjacent to the kinetochore (N = 30).

(E) Aurora B RNAi causes reduced sister centromere tension. Centromere-centromere distances in metaphase cells measured using ACA-ACA distance (N = 20 cells). Control RNAi, 1.34 $\pm$ 0.60 μm (N = 496); Aurora B RNAi 0.89 $\pm$ 0.45 μm (N = 270). Note that this latter value is significantly higher than that obtained in HeLa cells treated with taxol (Trinkle-Mulcahy et al., 2003), suggesting that tension is reduced, not eliminated.

reactivity across sister centromeres in mitosis, suggesting that phosphorylation of this site could be dynamic.

Phosphorylation at Ser186 occurs in the basic neck region of MCAK, a domain postulated to form a weak electrostatic interaction with the acidic C terminus of tubulin. The neck region may mediate diffusional motility of MCAK on the microtubule lattice (Hunter et al., 2003; Niederstrasser et al., 2002; Ovechkina et al., 2002). Phosphorylation of MCAK by Aurora B might therefore reduce the basic charge in this critical domain and thus disrupt key electrostatic interactions between MCAK and the carboxy-terminal tail of tubulin. Indeed, phosphorylation of MCAK by Aurora B inhibits MCAK microtubule depolymerization activity in vitro, and mimicking phosphorylation with point mutants inhibits depolymerization in vivo. Whether the four other phosphorylation sites we have identified all affect MCAK in the same way is not yet clear. In our in vivo microtubule depolymerization assay (Figure 4), EEEEE-MCAK showed less activity that any of the double or single S→E mutants. However, it seems likely that further biophysical and functional analyses will reveal separable functions of the individual sites.

The conservation of these Ser residues in other KinI's suggests a general mechanism for regulating the function of these enzymes. Indeed, a Ser or Thr residue is often C-terminal to the K-loop in several Kif1's, so phosphorylation may be a common mechanism for modulating K-loop function. Recently, the targeting of the chromosome-associated kinesin Kid has also been found to depend on phosphorylation (Ohsugi et al., 2003), suggesting that cell cycle-dependent posttranslational modification may be a common mechanism for targeting microtubule motors.

MCAK Phosphorylation Determines Localization to Centromeres and Kinetochores

Using two different approaches, we have identified distinct binding sites for MCAK at centromeres and kinetochores. In fixed cells, AAAAA-MCAK often localizes to a domain near the ACA antigen even in prometaphase, whereas the EEEEE-MCAK often remains in the inner centromere between ACA sites, even in metaphase cells (Figure 5E), suggesting that MCAK's phosphorylation status governs its preference for centromeres or kinetochores. Consistent with this, in living cells, we find that the FRAP recovery times of wtMCAK differ on aligned and unaligned chromosomes, which may mirror the localization differences between prometaphase and metaphase observed in fixed cells (Figure 1). AAAAA-MCAK recovers much more slowly than wtMCAK, suggesting a second binding site with different binding properties. In contrast, EEEEE-MCAK always recovers quickly, possibly reflecting this mutant's preference for occupancy of an inner centromere binding site, as observed in fixed cells (Figure 5E). Thus, the association of MCAK with different binding sites may depend on MCAK phosphorylation. ICIS, a recently discovered MCAK targeting factor, is likely to be the receptor for at least one of these sites (Ohi et al., 2003).

MCAK Phosphorylation in Biorientation and Mitosis

Aurora B is required for the establishment of bipolar orientation and may be involved in resolving syntelic attachments on mitotic chromosomes (Hauf et al., 2003; Tanaka et al., 2002). As disruption of MCAK function by microinjection of anti-MCAK antibodies (Kline-Smith and Walczak, 2002) or transfection of MCAK phosphorylation site mutants into mitotic cells (Figures 5A–5D) causes similar chromosome alignment defects as interfering with Aurora B function, it seems possible that Aurora B promotes biorientation and possibly syntelic resolution through MCAK. A major unresolved question is how Aurora B, MCAK, and ICIS collaborate to promote correct chromosome biorientation. Incorrect (e.g., syntelic) attachments may be selectively destabilized through MCAK's microtubule depolymerase activity. Alternatively, oscillatory chromosome movements driven through microtubule end depolymerization may help promote correct orientation. MCAK may be only one of many Aurora B targets involved in this process. Other studies have shown that disruption of Aurora B by RNAi, or by expression of Aurora B (KR), leads to loss of kinetochore CENP-E and cytoplasmic dynein (Murata-Hori et al., 2002), and to loss of kinetochore BubR1 and Mad2 (Ditchfield et al., 2003). Delocalization of MCAK from centromeres using an N-terminal dominant-negative fragment of MCAK does not affect CENP-E localization (Walczak et al., 2002), implying Aurora B separately directs the centromere targeting, and thus the function of MCAK and CENP-E. It therefore appears that Aurora B directs two separable pathways, one involving MCAK localization and function, and a second involving CENP-E and BubR1.

Protein Phosphorylation and Chromosome Dynamics

It is clear that the relative localization of Aurora B and MCAK changes during prometaphase (Figure 1). Furthermore, once attached to the mitotic spindle, chromosomes display dynamic oscillatory movement, indicating rapid changes in microtubule dynamics (Rieder and Salmon, 1994; Skibbens et al., 1993). We speculate that the relative positions of Aurora B and MCAK in the inner centromere and kinetochore could permit the switching of directional movement by asymmetrically altering local microtubule dynamics. Indeed, we find that Aurora B phosphorylates MCAK asymmetrically across metaphase centromeres (Figure 3G). This notion is attractive when one considers the recent discovery that protein phosphatase 1 (PP1), which antagonizes Aurora B (Hsu et al., 2000; Sassoon et al., 1999) and also regulates its activity (Murnion et al., 2001), is localized to the outer kinetochore in metaphase (Trinkle-Mulcahy et al., 2003). An additional level of control of depolymerizing activity may be afforded by modulating the affinity of MCAK for the different centromere/kinetochore binding sites through phosphorylation. The dynamic balance of phosphorylation of motors such as MCAK mediated by Aurora B and PP1 might then regulate the dynamic movements of chromosomes in the mitotic spindle. Moreover, it will be important to determine whether MCAK phosphorylation affects the dynamics of mono-oriented chromosomes in living cells.

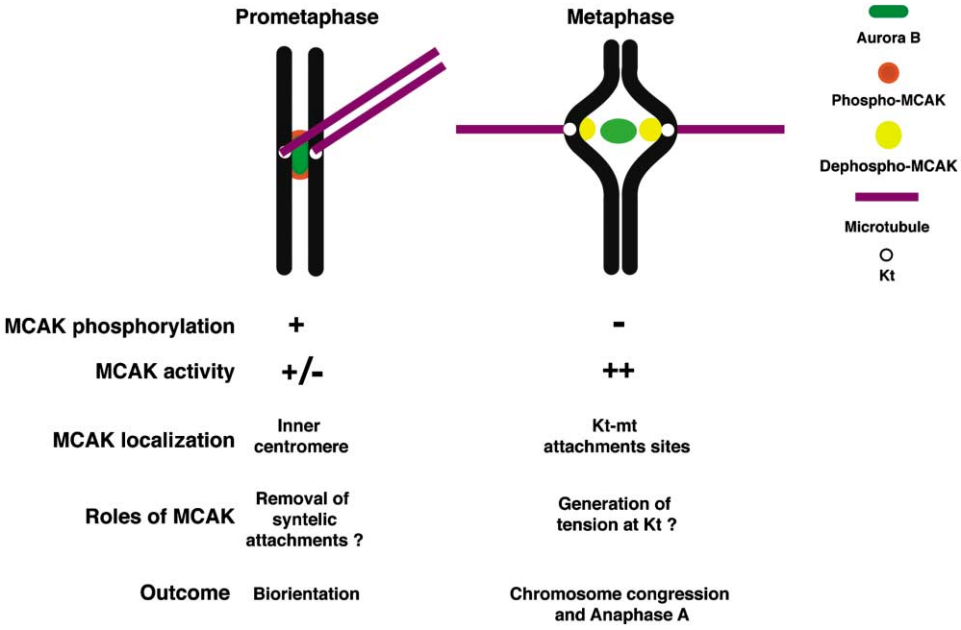

Figure 8. Model for the Regulation of MCAK by Aurora B in Mitosis

We propose a model for the role of Aurora B in regulating of MCAK activity during biorientation and throughout the process of chromosome congression, adapted from a previous suggestion (Tanaka et al., 2002). First, MCAK is targeted to the centromere by Aurora B phosphorylation. MCAK activity is inhibited by Aurora B phosphorylation, thereby increasing the probability that microtubule capture will result in stable kinetochore-microtubule interactions. MCAK activity is likely not completely inhibited, allowing it to destabilize incorrect (e.g., syntelic) attachments. After bipolar attachment initiates, the bioriented sister centromeres are under tension and the distance between them increases. MCAK separation from Aurora B favors its dephosphorylation, possibly by kinetochore-targeted PP1. Dephosphorylated MCAK would lose affinity for its inner-centromere binding site and gain affinity for its inner-kinetochore binding site concomitant with an increased catalytic activity, causing an increase in tension across the sister centromeres and full catalytic activity in anaphase.

Our finding that a phospho-mimic MCAK mutant is concentrated at the inner centromere and a nonphosphorylatable MCAK mutant is at the kinetochore, coupled with the observation that loss of Aurora B results in the appearance of MCAK on the spindle microtubules, suggests that inner-centromeric MCAK is phosphorylated and localized by its proximity to Aurora B in the absence of tension (Figure 8). At this point, MCAK activity is inhibited, possibly to prevent reversal of the initial microtubule-kinetochore attachments. Once bipolar attachment is established, MCAK and Aurora B are physically separated, MCAK phosphorylation decreases due to its proximity to PP1, and MCAK switches its affinity from centromeres to kinetochores/microtubule ends. Concomitantly, MCAK activity increases, allowing it to participate in force generation at the kinetochore. Whether this change in localization causes the MCAK microtubule depolymerase to switch from an error correction activity to a force generation machine can now be tested.

Experimental Procedures

Materials and Cell Culture

General laboratory reagents were purchased from Sigma or Merck. Microcystin-LR was the generous gift of Dr. C. MacKintosh (University of Dundee). HeLa cells were maintained in DMEM supplemented with 10% FBS (Sigma), 2 mM glutamate, and 10 U/ml Penicillin/Streptomycin at 37°C, 5% CO_2. Sheep anti-hamster MCAK polyclonal antiserum was produced via standard immunization and bleeding protocols (Pocono Rabbit Farm & Laboratory Inc., Canadensis, PA) using purified baculovirus-expressed hamster MCAK (Maney et al., 1998), affinity purified with immobilized bacterially expressed human MCAK (Ovechkina et al., 2002).

Immunofluorescence Microscopy

For immunofluorescence, cells grown on coverslips were fixed after washing once in 37°C PBS by incubation in 3.7% formaldehyde/PBS (pH 6.8) for 2 times 5 min at 37°C. Cells were permeabilized in PBS-0.1%Triton X-100 for 10 min at 37°C. Cells were blocked in AbDil (Cramer and Desai, 1995) supplemented with 0.1% normal donkey serum for 1 hr at room temperature. Anti-AIM1 (HsAurora B) monoclonal antibody (BD Biosciences) was used at 1:200 dilution. Affinity-purified sheep anti-human MCAK polyclonal antibody was diluted to 1 μg/ml. Rat anti-α-tubulin (Serotec) was used at a 1:500 dilution. Human CREST autoantisera (ACA; the generous gift of Professor Bill Earnshaw, University of Edinburgh) was diluted 1:10,000. All second antibodies (labeled with either FITC, Texas-Red, TRITC, or Cy5) were purchased from Jackson Laboratories.

3D data sets were acquired using a MicroMax cooled CCD camera (5 MHz: Roper Scientific), on a DeltaVision Restoration Microscope (Applied Precision, LLC, WA), built around a Nikon TE200 Eclipse stand with a 100 x/1.4NA PlanApo lens, or using a CoolSnap HQ cooled CCD camera on a DeltaVision Spectris Restoration Microscope built around an Olympus IX70 stand, with an a 100 x/1.4NA lens (Applied Precision, LLC, WA). Optical sections were recorded every 0.2 μm, and 3D data sets were deconvolved using the constrained iterative algorithm (Swedlow et al., 1997; Wallace et al., 2001) implemented in SoftWoRx software (Applied Precision LLC). Image data were quantified using SoftWoRx software. Kinetochore tubulin density was quantified in single optical sections using a 9 $\times$ 10 pixel box positioned at the plus end of kinetochore fibers. Integrated pixel intensities were measured for over 20 individual fibers in control and Aurora B RNAi cells. ACA-ACA distances were measured for clearly distinguishable metaphase centromere pairs lying along the pole-to-pole axis, using individual optical sections from 3D data sets from a large number of control and Aurora B RNAi cells.

Phospho-Specific Antibody Generation and Characterization

Phospho (ClQKQKRRS(Phos)VNSKIPA) and dephospho (ClQKQKR RSVNSKIPA) MCAK peptides encompassing the Ser92 phosphorylation site were synthesized and purified by Dr. G. Bloomberg (University of Bristol, UK). Phospho-Ser92 peptides were coupled to KLH (Calbiochem, UK) using standard protocols (Field et al., 1998) and used to immunize sheep (Diagnostics Scotland, UK). Phospho- and dephospho-peptides were coupled to Affigel 10 active ester agarose (BioRad) using iodoacetic acid N-Hydroxy-succinamide ester as described (Field et al., 1998). Serum was diluted 1:1 with TBS/0.1% Triton X-100, filtered, and repeatedly (5×) applied to a dephospho-peptide column. After washing with TBS and TBS/TX-100, antibodies were eluted with 0.2 M glycine (pH 2.6), and 0.1 M NaCl and immediately neutralized. Fractions containing antibody were pooled and dialyzed overnight against TBS. The flowthrough from the dephospho-peptide column was applied to the phospho-peptide column and then washed as above. Phospho-specific antibody was eluted as described above. For ELISA, serial dilutions (ranging from 100 μM to 0.001 μM; in 50 mM sodium carbonate buffer [pH 9.5]) of phospho-peptide, dephospho-peptide, or control Histone H3 serine 10 peptide were coated onto 96-well plates washed extensively (PBS, 0.05% Tween 20), blocked with 0.1% BSA/PBS, and washed (PBS, 0.05% Tween 20), and then diluted purified antiserum (1 μg/ml) was added to each well for 2 hr at room temperature. Bound antibody was detected with diluted (1:5000) anti-sheep-HRP conjugate and TMB solution (Sigma). Assay was read at 450 nm in a plate reader. To pre-block antibody with either the phospho-peptides or dephospho-peptide, 1 μg antibody was incubated with 0.5 mM peptide on ice for 1 hr prior to its addition to the ELISA. The antibodies were tested by Western blotting recombinant MCAK that had previously been either mock phosphorylated or phosphorylated by recombinant Ipl1p/Sli15p. Antibody specificity was similarly tested in fixed HeLa cells by preblocking antibody (10 μg Ab with 5 mM peptide).

Fluorescence Recovery after Photobleaching

Fluorescence recovery after photobleaching (FRAP) on wild-type and phosphorylation site mutant GFP-MCAK was performed on HeLa cells 18–24 hr after transfection with GFP-wtMCAK and GFP-AAAAA-MCAK and GFP-EEEEE-MCAK plasmids. All experiments were conducted using a FRAP-enabled DeltaVision Spectris (as above) fitted with a 10 mW 488 nm solid-state laser. The laser was focused to a diffraction-limited spot and spot bleaching performed with a single 50 ms stationary pulse at 90% laser power. The first image was acquired approximately 50 ms after the bleach event. For the first second, images were acquired every 150 ms, for the following 2 s every 300 ms, then at 800 ms intervals in the following 8 s, after which images were acquired every 1.5 s for the remainder of the experiment. Recovery models were generated and half-times calculated using the method of Axelrod (Axelrod et al., 1976) as implemented within SoftWoRx software. Centromeres were individually targeted for photobleaching and categorized as either aligned (congressed) or unaligned (noncongressed).

Aurora B Kinase Isolation, In Vitro Phosphorylation, and Phosphorylation Site Identification

Mitotic and interphase chromatin eluates (MCE and ICE, respectively) were prepared from in vitro-assembled *Xenopus* (Murnion et al., 2001; Swedlow, 1999) and used as a source of cell cycle-regulated Aurora B kinase activity. Aurora B complex was immunoprecipitated from MCE or ICE using an affinity-purified rabbit anti-Xaurora B polyclonal antibody raised against a peptide (CTTPSSATAAQRVL-RKEP) in the N terminus of *Xenopus* Aurora B conjugated to KLH (Field et al., 1998). This antibody recognizes a single band on Western blots and immunoprecipitates active Aurora B-INCENP complex from MCE and inactive Aurora B-INCENP complex from ICE (Murnion et al., 2001; data not shown). Control immunoprecipitations were performed in parallel using normal rabbit IgG bound to Affiprep Protein A beads. Bacterially expressed and purified Ipl1p-GST and Sli15p-GST were the generous gifts of N. Rachidi, University of Dundee. For in vitro phosphorylation studies, 2–4 μl Aurora B kinase beads were incubated with 0.2 μg recombinant hamster MCAK (Maney et al., 2001), in a 20 μl reaction buffer containing 2 μl [γ-^{32}P] ATP (10 mCi/ml: specific activity > 5000 Ci/mmol), 0.2 mM cold ATP, 1 x XBE2, 5 mM $MgCl_2$, and 1 μM Microcystin-LR, for 1 hr at 22°C, with shaking. Kinase reactions were terminated with Laemmli sample buffer, heated to 70°C for 5 min, and subjected to SDS-PAGE. After electrophoresis, gels were stained with Coomassie and destained and MCAK bands were excised. Phosphorylation site analysis was performed (Lizcano et al., 2002), except for the use of LysC for enzymatic digestion in order to determine MCAK phosphorylation sites more readily.

2D Gel Electrophoresis

To detect modification of human MCAK in Aurora B/control RNAi-treated HeLa cells (see below for details), whole-cell extracts (Feijoo et al., 2001) were prepared in the presence of phosphatase inhibitors, TCA precipitated, and rehydrated in sample buffer supplemented with 50 mM DTT and appropriate ampholytes. Isoelectric focusing was performed overnight using a BioRad Protean IEF Cell System, employing pH 6–11 Immobiline DryStrip isoelectric focusing strips (Amersham PLC). Proteins were separated in the second dimension on NuPAGE 4%–12% Bis-Tris IPG gels (Novex) run in MOPS buffer (Novex). 2D gels were blotted onto Protrans nitrocellulose membrane (Schleicher and Schuell). ECL was used for immunoblot detection (Amersham, PLC).

Microtubule Depolymerization Assays

Baculovirus-expressed 6His-hamster MCAK (Maney et al., 1998) was phosphorylated by incubation at 22°C for 90 min in 20 μl of 8 mM K-HEPES (pH 7.7), 65 mM KCl, 40 mM sucrose, 6 mM $MgCl_2$, 4 mM K-EGTA (pH 7.7), 60 mM Imidazole, 1 mM DTT, 0.2 mM ATP, 1 μM Microcystin-LR (Sigma), and 0.03% Triton X-100 in the presence of Aurora B complexes precipitated with rabbit α-Aurora B Ab-protein A-agarose beads (or rabbit IgG-protein A-agarose beads). Microtubule depolymerization was performed as described previously (Maney et al., 2001; Ovechkina et al., 2002). pEGFP-CgMCAK (pYOY71) was made by subcloning of BspE1-HindIII CgMCAK cDNA into pEGFP-C1 vector (Clontech). CgMCAK mutants were made by overlapping PCR mutagenesis using PfuTurbo DNA polymerase (Stratagene) and sequenced. CHO cells were cultured and transfected as described previously (Maney et al., 2001; Ovechkina et al., 2002).

Transfection and Imaging of Aurora B (KR)

Rat Aurora B and Aurora B (KR) were excised from GFP-Aurora B and GFP-Aurora B (KR) (a kind gift of Yu-Li Wang) and ligated into ECFP-N1 (Clontech). Full-length hamster MCAK was excised from pYOY71 (described above) and ligated into EYFP-C1 (Clontech). Motorless MCAK was excised from GFP-ML-MCAK (Maney et al., 1998) and ligated to EYFP-C1 (Clontech). CHO cells were cotransfected with CFP-Aurora or CFP-Aurora B (KR) in combination with either YFP-MCAK or YFP-ML MCAK. The cells were cultured for 16 hr, fixed in 1% glutaraldehyde in PBS for 20 min, and reduced in 5% $NaBH_4$/PBS for 20 min. Microtubules were labeled with DM1 (Sigma) and Texas Red-conjugated secondary antibodies.

RNAi

A 21 nt siRNA (AAGAGCCUGUCACCCCAUCUG: Dharmacon Research Inc., USA) corresponding to position +149 → +169 of the human Aurora B (STK12) coding sequence was used for Aurora B RNAi, depleting Aurora B protein levels by more than 75% in less than 24 hr. Lamin A/C siRNA and a scrambled random siRNA duplex (Dharmacon Research, Inc.) were used as controls. For RNAi, HeLa cells were seeded onto 13 mm coverslips and grown overnight in medium without antibiotics. Transfection was performed using Oligofectamine (Invitrogen, Inc.) using 60 pmol siRNA per well following manufacturer's protocols. Coverslips were fixed at intervals between 5 and 48 hr posttransfection and processed for immunofluorescence. The siRNA duplex used significantly decreases Aurora B protein levels within 10 to 24 hr in single cells (data not shown). Previously, we have characterized the dynamic range of our microscope system and shown that we can accurately measure relative intensities over ~2.5 orders of magnitude with a coefficient of variation of ~6%–9% (Swedlow et al., 2002). We have used this capability to accurately measure the depletion of Aurora B, as detected by

immunofluorescence and score phenotypes in single cells with Aurora B levels <1% of control cells. The mean depletion of Aurora B assayed by quantifying fluorescence in single cells was 76.9 ± 19.6% (N = 15; also see Supplemental Figure S2), which was similar to the value obtained from immunoblots of whole-cell lysates, suggesting that immunofluorescence, at least in this case, can be used to quantify Aurora B levels in fixed cells. Images for Aurora B RNAi and control RNAi cells were acquired and processed under identical conditions. For analysis of protein levels on 2D gels, the RNAi treatment was scaled up using 900 pmol siRNA duplexes.

Acknowledgments

We thank Bill Earnshaw for the ACA antibody, Yu-Li Wang for the kinase-dead Aurora B, Najma Rachidi for Ipl1p/Sli15p and many useful discussions, Iain Porter and Guennadi Khodouli for assistance with 2D gels, past and present members of Swedlow lab for help with *Xenopus* extracts, and Tomo Tanaka for critical reading of the manuscript and many thoughtful discussions. This work was supported by grants from the Wellcome Trust and Cancer Research UK (to J.R.S.) and from the Department of Defense (DAMD17-01-1-0450) (to L.W). J.R.S. is a Wellcome Trust Senior Research Fellow.

Received: May 23, 2003
Revised: August 22, 2003
Accepted: December 11, 2003
Published: February 9, 2004

References

Adams, R.R., Maiato, H., Earnshaw, W.C., and Carmena, M. (2001). Essential roles of *Drosophila* inner centromere protein (INCENP) and Aurora B in histone h3 phosphorylation, metaphase chromosome alignment, kinetochore disjunction, and chromosome segregation. J. Cell Biol. *153*, 865–880.

Andrews, P.D., Knatko, E., Moore, W.J., and Swedlow, J.R. (2003). Mitotic mechanics: the Auroras come into view. Curr. Opin. Cell Biol. *15*, 672–683.

Axelrod, D., Koppel, D.E., Schlessinger, J., Elson, E., and Webb, W.W. (1976). Mobility measurement by analysis of fluorescence photobleaching recovery kinetics. Biophys. J. *16*, 1055–1069.

Biggins, S., Severin, F.F., Bhalla, N., Sassoon, I., Hyman, A.A., and Murray, A.W. (1999). The conserved protein kinase Ipl1 regulates microtubule binding to kinetochores in budding yeast. Genes Dev. *13*, 532–544.

Carmena, M., and Earnshaw, W.C. (2003). The cellular geography of Aurora kinases. Nat. Rev. Mol. Cell Biol. *4*, 842–854.

Cheeseman, I.M., Anderson, S., Jwa, M., Green, E.M., Kang, J., Yates, J.R., 3rd, Chan, C.S., Drubin, D.G., and Barnes, G. (2002). Phospho-regulation of kinetochore-microtubule attachments by the Aurora kinase Ipl1p. Cell *111*, 163–172.

Cramer, L., and Desai, A. (1995). (http://mitchison.med.harvard.edu/protocols/gen1.html).

Desai, A., Verma, S., Mitchison, T.J., and Walczak, C.E. (1999). Kin I kinesins are microtubule-destabilizing enzymes. Cell *96*, 69–78.

Ditchfield, C., Johnson, V.L., Tighe, A., Ellston, R., Haworth, C., Johnson, T., Mortlock, A., Keen, N., and Taylor, S.S. (2003). Aurora B couples chromosome alignment with anaphase by targeting BubR1, Mad2, and Cenp-E to kinetochores. J. Cell Biol. *161*, 267–280.

Feijoo, C., Hall-Jackson, C., Wu, R., Jenkins, D., Leitch, J., Gilbert, D.M., and Smythe, C. (2001). Activation of mammalian Chk1 during DNA replication arrest: a role for Chk1 in the intra-S phase checkpoint monitoring replication origin firing. J. Cell Biol. *154*, 913–923.

Field, C.M., Oegema, K., Zheng, Y., Mitchison, T.J., and Walczak, C.E. (1998). Purification of cytoskeletal proteins using peptide antibodies. Methods Enzymol. *298*, 525–541.

Giet, R., and Glover, D.M. (2001). *Drosophila* Aurora B kinase is required for histone H3 phosphorylation and condensin recruitment during chromosome condensation and to organize the central spindle during cytokinesis. J. Cell Biol. *152*, 669–682.

Hauf, S., Cole, R.W., LaTerra, S., Zimmer, C., Schnapp, G., Walter, R., Heckel, A., Van Meel, J., Rieder, C.L., and Peters, J.M. (2003). The small molecule Hesperadin reveals a role for Aurora B in correcting kinetochore-microtubule attachment and in maintaining the spindle assembly checkpoint. J. Cell Biol. *161*, 281–294.

He, X., Rines, D.R., Espelin, C.W., and Sorger, P.K. (2001). Molecular analysis of kinetochore-microtubule attachment in budding yeast. Cell *106*, 195–206.

Homma, N., Takei, Y., Tanaka, Y., Nakata, T., Terada, S., Kikkawa, M., Noda, Y., and Hirokawa, N. (2003). Kinesin superfamily protein 2A (KIF2A) functions in suppression of collateral branch extension. Cell *114*, 229–239.

Hsu, J.-Y., Sun, Z.-W., Li, X., Reuben, M., Tatchell, K., Bishop, D.K., Grushcow, J.M., Brame, C.J., Caldwell, J.A., Hunt, D.F., et al. (2000). Mitotic phosphorylation of histone H3 is governed by Ipl1/aurora kinase and Glc7/PP1 phosphatase in budding yeast and nematodes. Cell *102*, 279–291.

Hunter, A.W., and Wordeman, L. (2000). How motor proteins influence microtubule polymerization dynamics. J. Cell Sci. *113*, 4379–4389.

Hunter, A.W., Caplow, M., Coy, D.L., Hancock, W.O., Diez, S., Wordeman, L., and Howard, J. (2003). The kinesin-related protein MCAK is a microtubule depolymerase that forms an ATP-hydrolyzing complex at microtubule ends. Mol. Cell *11*, 445–457.

Kaitna, S., Mendoza, M., Jantsch-Plunger, V., and Glotzer, M. (2000). Incenp and an aurora-like kinase form a complex essential for chromosome segregation and efficient completion of cytokinesis. Curr. Biol. *10*, 1172–1181.

Kang, J.S., Cheeseman, I.M., Kallstrom, G., Velmurugan, S., Barnes, G., and Chan, C.S. (2001). Functional cooperation of Dam1, Ipl1, and the inner centromere protein (INCENP)-related protein Sli15 during chromosome segregation. J. Cell Biol. *155*, 763–774.

Kline-Smith, S.L., and Walczak, C.E. (2002). The microtubule-destabilizing kinesin XKCM1 regulates microtubule dynamic instability in cells. Mol. Biol. Cell *13*, 2718–2731.

Lizcano, J.M., Deak, M., Morrice, N., Kieloch, A., Hastie, C.J., Dong, L., Schutkowski, M., Reimer, U., and Alessi, D.R. (2002). Molecular basis for the substrate specificity of NIMA-related kinase-6 (NEK6). Evidence that NEK6 does not phosphorylate the hydrophobic motif of ribosomal S6 protein kinase and serum- and glucocorticoid-induced protein kinase in vivo. J. Biol. Chem. *277*, 27839–27849.

Maney, T., Hunter, A.W., Wagenbach, M., and Wordeman, L. (1998). Mitotic centromere-associated kinesin is important for anaphase chromosome segregation. J. Cell Biol. *142*, 787–801.

Maney, T., Wagenbach, M., and Wordeman, L. (2001). Molecular dissection of the microtubule depolymerizing activity of mitotic centromere-associated kinesin. J. Biol. Chem. *276*, 34753–34758.

Murata-Hori, M., and Wang, Y.L. (2002). The kinase activity of Aurora B is required for kinetochore-microtubule interactions during mitosis. Curr. Biol. *12*, 894–899.

Murata-Hori, M., Tatsuka, M., and Wang, Y.L. (2002). Probing the dynamics and functions of aurora B kinase in living cells during mitosis and cytokinesis. Mol. Biol. Cell *13*, 1099–1108.

Murnion, M.E., Adams, R.A., Callister, D.M., Allis, C.D., Earnshaw, W.C., and Swedlow, J.R. (2001). Chromatin-associated protein phosphatase 1 regulates aurora-B and histone H3 phosphorylation. J. Biol. Chem. *276*, 26656–26665.

Niederstrasser, H., Salehi-Had, H., Gan, E.C., Walczak, C., and Nogales, E. (2002). XKCM1 acts on a single protofilament and requires the C terminus of tubulin. J. Mol. Biol. *316*, 817–828.

Ohi, R., Coughlin, M.L., Lane, W.S., and Mitchison, T.J. (2003). An inner centromere protein that stimulates the microtubule depolymerizing activity of a KinI kinesin. Dev. Cell *5*, 309–321.

Ohsugi, M., Tokai-Nishizumi, N., Shiroguchi, K., Toyoshima, Y.Y., Inoue, J., and Yamamoto, T. (2003). Cdc2-mediated phosphorylation of Kid controls its distribution to spindle and chromosomes. EMBO J. *22*, 2091–2103.

Ovechkina, Y., Wagenbach, M., and Wordeman, L. (2002). K-loop insertion restores microtubule depolymerizing activity of a "neckless" MCAK mutant. J. Cell Biol. *159*, 557–562.

Rieder, C.L., and Salmon, E.D. (1994). Motile kinetochores and polar ejection forces dictate chromosome position on the vertebrate mitotic spindle. J. Cell Biol. *124*, 223–233.

Sassoon, I., Severin, F.F., Andrews, P.D., Taba, M.R., Kaplan, K.B., Ashford, A.J., Stark, M.J., Sorger, P.K., and Hyman, A.A. (1999). Regulation of *Saccharomyces cerevisiae* kinetochores by the type 1 phosphatase Glc7p. Genes Dev. *13*, 545–555.

Skibbens, R.V., Skeen, V.P., and Salmon, E.D. (1993). Directional instability of kinetochore motility during chromosome congression and segregation in mitotic newt lung cells: a push-pull mechanism. J. Cell Biol. *122*, 859–875.

Swedlow, J.R. (1999). Chromosome assembly in vitro using Xenopus egg extracts. In Chromosome Structural Analysis, W.A. Bickmore, ed. (Oxford: Oxford), pp. 167–182.

Swedlow, J.R., Sedat, J.W., and Agard, D.A. (1997). Deconvolution in optical microscopy. In Deconvolution of Images and Spectra, P.A. Jansson, ed. (New York: Academic Press), pp. 284–309.

Swedlow, J.R., Hu, K., Andrews, P.D., Roos, D.S., and Murray, J.M. (2002). Measuring tubulin content in *Toxoplasma gondii*: a comparison of laser-scanning confocal and wide-field fluorescence microscopy. Proc. Natl. Acad. Sci. USA *99*, 2014–2019.

Tanaka, T.U., Rachidi, N., Janke, C., Pereira, G., Galova, M., Schiebel, E., Stark, M.J.R., and Nasmyth, K. (2002). Evidence that the Ipl1-Sli15 (Aurora kinase-INCENP) complex promotes chromosome bi-orientation during mitosis by altering kinetochore-spindle pole connections. Cell *108*, 317–329.

Trinkle-Mulcahy, L., Andrews, P.D., Wickramasinghe, S., Sleeman, J., Prescott, A., Lam, Y.W., Lyon, C., Swedlow, J.R., and Lamond, A.I. (2003). Time-lapse imaging reveals dynamic relocalization of PP1gamma throughout the mammalian cell cycle. Mol. Biol. Cell *14*, 107–117.

Walczak, C.E., Mitchison, T.J., and Desai, A. (1996). XKCM1—a Xenopus kinesin-related protein that regulates microtubule dynamics during mitotic spindle assembly. Cell *84*, 37–47.

Walczak, C.E., Gan, E.C., Desai, A., Mitchison, T.J., and Kline-Smith, S.L. (2002). The microtubule-destabilizing kinesin XKCM1 is required for chromosome positioning during spindle assembly. Curr. Biol. *12*, 1885–1889.

Wallace, W., Schaefer, L.H., and Swedlow, J.R. (2001). A workingperson's guide to deconvolution in light microscopy. Biotechniques *31*, 1076–1097.

Waters, J.C., Skibbens, R.V., and Salmon, E.D. (1996). Oscillating mitotic newt lung cell kinetochores are, on average, under tension and rarely push. J. Cell Sci. *109*, 2823–2831.

Westermann, S., Cheeseman, I.M., Anderson, S., Yates, J.R., 3rd, Drubin, D.G., and Barnes, G. (2003). Architecture of the budding yeast kinetochore reveals a conserved molecular core. J. Cell Biol. *163*, 215–222.

Wordeman, L., Wagenbach, M., and Maney, T. (1999). Mutations in the ATP-binding domain affect the subcellular distribution of mitotic centromere-associated kinesin (MCAK). Cell Biol. Int. *23*, 275–286.

Zeitlin, S.G., Shelby, R.D., and Sullivan, K.F. (2001). CENP-A is phosphorylated by Aurora B kinase and plays an unexpected role in completion of cytokinesis. J. Cell Biol. *155*, 1147–1157.